Check for updates

Chemistry–A European Journal
Research Article
doi.org/10.1002/chem.202400389
Chemistry Europe
European Chemical Societies Publishing
www.chemeurj.org



# Synthesis, Reactivity, and Complexation with Fe(0) of a Tight-bite Bis(N-heterocyclic silylene)

Zohreh Hendi[+],[a] Madhusudan K. Pandey[+],[a] Katharina Rachuy,[a] Mukesh K. Singh,[b] Regine Herbst-Irmer,[a] Dietmar Stalke,*[a] and Herbert W. Roesky*[a]

The synthesis, reactivity, and complexation with Fe(0) precursor of a tight-bite bis(N-heterocyclic silylene) (bis(NHSi)) ligand **1** are reported. The reaction of **1** with *p*-toluidine led to the activation of both N–H bonds across Si(II) atoms to afford a four-membered heterocyclic cyclodisilazane **2**, with hydride substituents attached to five-coordinate Si atoms. A 1:2 reaction of **1** with $Fe(CO)_5$ led to an intriguing dinuclear complex **3** featuring a five-membered (N–Si–Fe–Fe–Si) ring with a Fe–Fe bond distance of 2.6892(13) Å. All compounds (**1**-**3**) were thoroughly characterized by various spectroscopic methods and X-ray diffraction studies conclusively established their molecular structures. DFT calculations were carried out to shed light on bonding and energetic aspects in **1**–**3**.

## Introduction

Silylenes, once considered laboratory curiosities, are now one of the most thoroughly studied classes of compounds in main-group chemistry. A lone pair of electrons and a vacant 3p orbital at the Si(II) atom allow them to function as Lewis bases as well as Lewis acids.[1] West and Denk isolated the first example of stable N-heterocyclic silylene (NHSi) in 1994, which marked the beginning of a new era in silylene chemistry.[2] Since then, several stable silylenes have been synthesized, and their reactivity has been explored in various fields of chemistry.[1b,3] However, silylene chemistry got a major breakthrough when Roesky and co-workers isolated the first heteroleptic chlorosilylene [(PhC(N$^t$Bu)$_2$SiCl], marking the start of a burgeoning era in silylene chemistry.[4] Due to the readily functionalizable Si–Cl bond, the heteroleptic chlorosilylene led to several functionalized silylenes, widely applied in main-group chemistry and catalysis. Notably, bissilylenes obtained from chlorosilylene are versatile compounds for stabilizing low-valent elements of the main group, activating small molecules, and synthesizing silicon-incorporated heterocycles, which were inaccessible otherwise.[1c,5] Bissilylenes are classified into two types: (i) interconnected and (ii) spacer-separated bissilylenes (Figure 1).[6]

In the spacer-separated bissilylenes, the silicon atoms feature the oxidation states of +2, and the reactivity is based on their lone pair of electrons. Whereas Si in interconnected bissilylenes is in the +1 oxidation state, and the reactivity is based on both, a lone pair of electrons at the silicon atoms as well as the labile sigma bond between them. In the spacer-separated bis-silylene the distance between silicon atoms plays a crucial role in their reactivity. Driess and co-workers demonstrated that smaller elements can be stabilized with spacer-

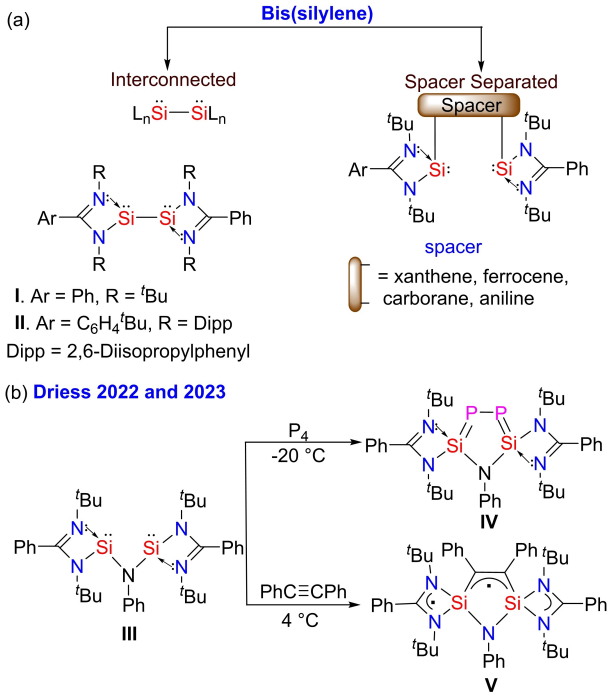



**Figure 1.** (a) Amidinate stabilized bis-silylene ligands. (b) Driess bis(NHSi) **III** and its reactivity studies

[a] Dr. Z. Hendi,[+] Dr. M. K. Pandey,[+] K. Rachuy, Dr. R. Herbst-Irmer, D. Stalke, Dr. H. W. Roesky
Institut für Anorganische Chemie
Georg-August-Universität Göttingen
Göttingen, 37077, Germany
E-mail: hroesky@gwdg.de
dstalke@chemie.uni-goettingen.de

[b] Dr. M. K. Singh
School of Chemistry,
University of Edinburgh
Edinburgh, EH9 3FJ, United Kingdom

[+] These authors contributed equally.

Supporting information for this article is available on the WWW under https://doi.org/10.1002/chem.202400389

© 2024 The Authors. Chemistry - A European Journal published by Wiley-VCH GmbH. This is an open access article under the terms of the Creative Commons Attribution License, which permits use, distribution and reproduction in any medium, provided the original work is properly cited.


© 2024 The Authors. Chemistry - A European Journal published by Wiley-VCH GmbH

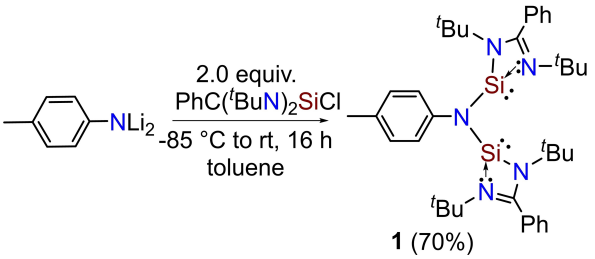
separated bissilylenes with smaller Si···Si distances.[1c] Very recently, a new type of spacer-separated bis(NHSi) **III** (Figure 1), which is the silicon(II) analogue to well-known bisaminophosphanes, was developed by Driess and co-workers.[7] The reaction of **III** with $P_4$ led to the formation of a rare 2,5-disila-3,4-diphosphapyrrole (**IV**). In contrast, diphenyl acetylene resulted in the formation of an unusual diradical (**V**) at 4 °C and an interesting cyclotetramer at room temperature.[8] With this knowledge, we hypothesized that bissilylenes with short Si···Si distances might help activate the challenging bonds and might also afford the M–M bonded compounds upon treatments with suitable precursors. Herein we report bis(NHSi) **1** using *p*-toluidine as a spacer and its reactivity with *p*-toluidine and $Fe(CO)_5$. The details are described.

## Results and Discussion

### Synthesis and Characterization of the Bis(NHSi) (1)

Compound **1** was synthesized similarly to the procedure developed by Driess and co-workers.[7] The reaction of *in situ* generated dilithiated amide $ArNLi_2$ (Ar = *p*-toluidine) with heteroleptic chlorosilylene [(PhC(N$^t$Bu)$_2$SiCl] in 1:2 molar ratios afforded the desired bis(NHSi) compound **1** in good yield (Scheme 1).

The $^{29}$Si NMR spectrum of **1** (Figure S2) showed a singlet resonance at −12.2 ppm, which is significantly upfield shifted (25 ppm) compared to the starting chlorosilylene compound [(PhC(N$^t$Bu)$_2$SiCl] (14 ppm) and is similar to the same reported for analogous bis(NHSi) compound reported by Driess and co-workers (−12.9 ppm).[7] The LIFDI mass spectrum of **1** showed $[M]^+$ at 623.4 (m/z = 623.3839), suggesting the anticipated compound formation. Compound **1** (Figure 2) crystallized in the monoclinic space group *C2/c* with one molecule in the asymmetric unit (see SI: Table S1).[9] The Si–N–Si angle of 109.33(8)° in **1** and the intramolecular Si$^{II}$···Si$^{II}$ distance in **1** amounts to 2.8864(9) Å, akin to that in Ph-$NSi_2$ (Si–N–Si angle: 109.4(1)° and Si$^{II}$···Si$^{II}$ distance 2.895(1) Å).[7]




**Scheme 1.** Synthesis of bis(NHSi) **1**.

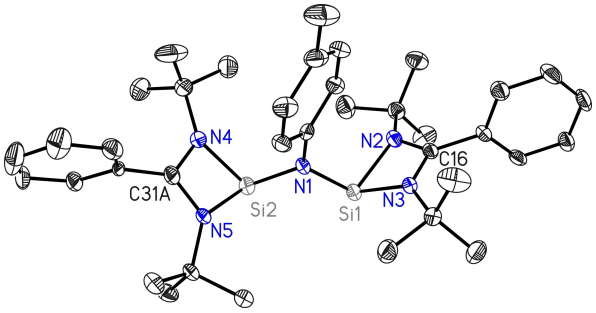



**Figure 2.** Molecular structure of **1**. The anisotropic displacement parameters are depicted at the 50% probability level. Hydrogen atoms have been omitted for clarity. Selected bond lengths (Å) and bond angles (°). Si1–Si2 2.8864(9), Si1–N1 1.7693(16), Si2–N1 1.7688(16), Si1–N2 1.8901(16), Si1–N3 1.8785(16), Si2–N4 1.8752(17), Si2–N5 1.9081(16), Si2–N1–Si1 109.33(8), N2–Si1–N3 68.86(7), N1–Si1–N2 106.50(7), N3–Si1–N1 102.93(7), N4–Si2–N5 68.68(7), N4–Si2–N1 103.29(7), N5–Si2–N1 106.76(7).

N–H bond activation is a crucial transformation in organic synthesis due to its significance in several industrial processes.[10] Nevertheless, transition metal-catalyzed "N–H activation" reactions are challenging due to the propensity of amines to form Werner-type complexes.[10a,11] Recently it has been observed that low-valent elements of the main group could activate N–H bonds, forming amido/hydride derivatives.[12] The reactivity studies of silylenes with organic compounds generally proceed with the oxidation from formally divalent to thermodynamically stable tetravalent states.[13] However, the N–H bond activation *via* oxidative addition is challenging and only scarcely studied with silylenes (Figure 3).[14]

Roesky and co-workers were the first to utilize silylene for the activation of N–H bonds in ammonia and alkylhydrazine to give Si(H)(NHR) derivatives (**VII**–**IX**).[14a] Following this, Aldridge and co-workers utilized an acyclic silylene **X** for the ammonia activation reaction.[14b] Very recently, the same group utilized a cationic silylene for the activation of $^t$BuNH$_2$ to afford **XIII**.[14c] A

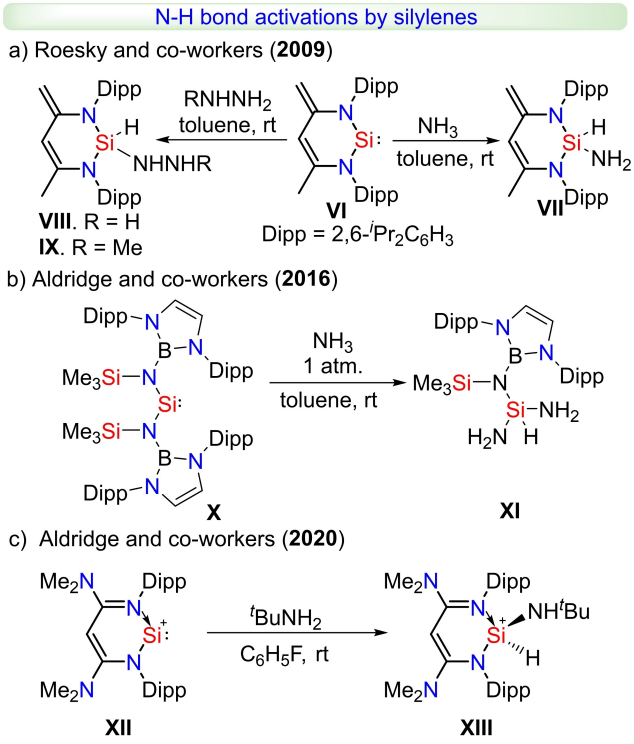
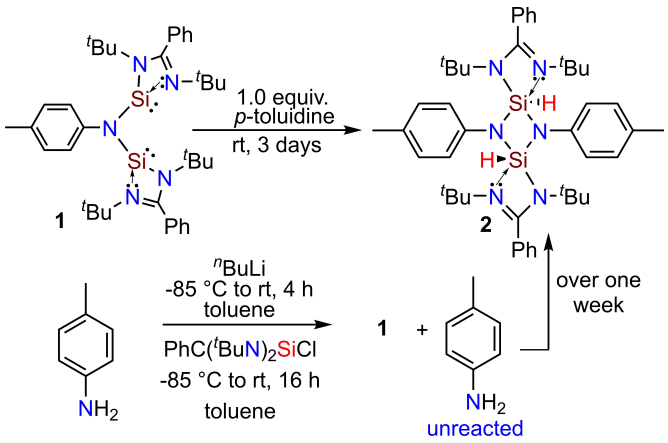



**Figure 3.** Selected examples of N–H bond activation by silylenes.


© 2024 The Authors. Chemistry - A European Journal published by Wiley-VCH GmbH

15213765, 2024, 31, Downloaded from https://chemistry-europe.onlinelibrary.wiley.com/doi/10.1002/chem.202400389, Wiley Online Library on [07/11/2026]. See the Terms and Conditions (https://onlinelibrary.wiley.com/terms-and-conditions) on Wiley Online Library for rules of use; OA articles are governed by the applicable Creative Commons License

low-lying unoccupied 3p orbital in these systems facilitates the coordination of substrates (amines) rather than activation of N–H bonds, as observed similarly with transition metals. However, it has been shown that subsequent proton transfer from nitrogen to an electrophilic silicon atom affords the Si(H)(NHR) derivatives.[13,15] While the cleavage of N–H bonds has been documented by Si(II) compounds, the activation of both N–H bonds of an amine to produce heterocyclic compounds remains unexplored. It is worth noting that activating both N–H bonds using low-valent elements is a significant approach for creating highly complex heterocycles that contain main-group elements. Considering this, we aimed to examine the reaction of *p*-toluidine with bis(NHSi) **1** to determine the resulting product. Remarkably, the reaction of **1** with an equal amount of *p*-toluidine (Scheme 2) resulted in the simultaneous activation of both N–H bonds by both silicon(II) atoms. This led to the formation of a four-membered heterocyclic cyclodisilazane compound **2**, which contains N–SiH–N–SiH atoms. In an attempt to stabilize a reactive -NH function next to Si(II), we tried to metalate *p*-toluidine first with one equivalent of $^{n}$BuLi, followed by the addition of one equivalent of [(PhC(N$^{t}$Bu)$_2$SiCl]. Interestingly, this resulted in the formation of **2** instead of the aminosilylene target compound.




**Scheme 2.** Synthesis of compound (**2**).

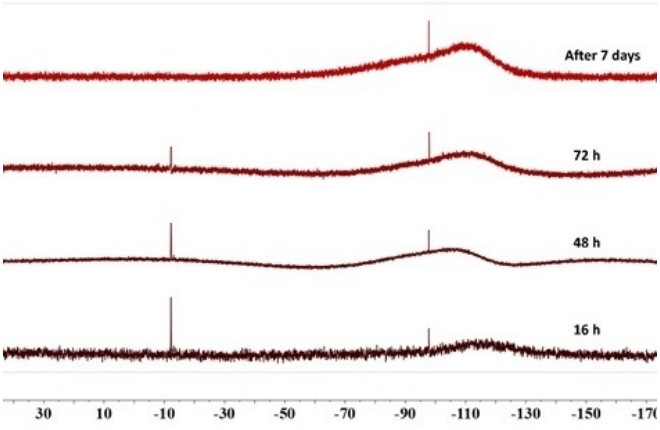



**Figure 4.** Stack plot of $^{29}$Si NMR spectra showing complete formation of compound **2** in 7 days.

This might be due to the facile dilithiation of *p*-toluidine with $^{n}$BuLi[16] leading to *in situ* generation of half equivalent of bis(NHSi) **1**, which further reacts slowly (over one week) with half of the unreacted *p*-toluidine to afford **2** (Figure 4). The $^{1}$H and $^{29}$Si NMR spectra and the unit cell of the crystals obtained from these two reactions are completely identical, confirming this outcome.

The $^{1}$H NMR spectrum of **2** in $C_6D_6$ showed a characteristic Si–H resonance at 6.20 ppm, which is similar to the same reported for a five coordinated donor-stabilized Si–H compound reported from our group (6.34 ppm) and is slightly downfield shifted compared to the five coordinated N-substituted hydrosila hydrazone (4.86 ppm) and four coordinated Si–H resonance in 1,3-bis(silyl)cyclodisilazane (5.45 ppm).[17] Whereas, the aromatic protons appeared in the range of 6.96–7.59 ppm.

The $^{t}$Bu protons appeared as two broad singlets in the range of 0.75 to 1.29 ppm, this might be due to the very facile flipping of the two N$^{t}$Bu groups of amidinate backbone around the Si center at room temperature. As can be seen from the X-ray structure (*vide infra*), one of the Si–N bonds is longer (2.0060(12) Å) than the other (1.8265(12) Å); this suggests that such flipping of the N$^{t}$Bu group is possible. However, when the $^{1}$H NMR spectrum was measured at −30 °C in THF-$D_8$, both the N$^{t}$Bu protons appeared as sharp singlets (see SI: Figure S7) suggesting that the flipping of N$^{t}$Bu group is very facile at room temperature and as a result an averaged signal was observed.

The $^{29}$Si NMR spectrum of **2** (Figure S8) showed a singlet peak at −97 ppm, which is upfield shifted compared to the same in **1**, and is comparable to that of a five-coordinated silicon compound, and is also in agreement with the oxidation of silicon(II) to silicon(IV) in **2**.[17b–c,18] The LIFDI mass spectrum showed [M]$^{+}$ peak at 730.3 (m/z = 730.0303) with high intensity further substantiating the formation of **2**. The solid-state structure of **2** is shown in Figure 5. It crystallizes in the triclinic

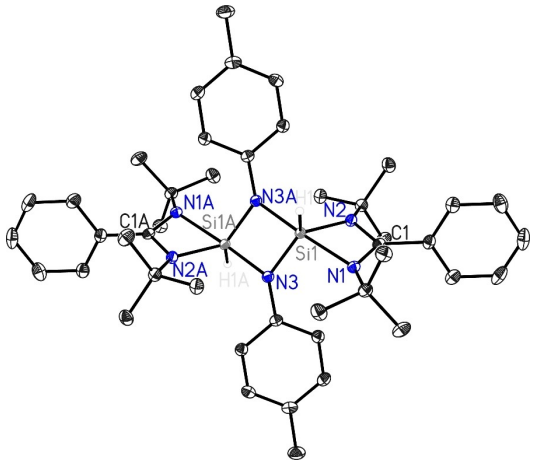



**Figure 5.** Molecular structure of **2**. The anisotropic displacement parameters are depicted at the 50% probability level. Hydrogen atoms, except SiH, have been omitted for clarity. Selected bond lengths (Å) and bond angles (°). Si1–Si1A 2.6546(9), Si1-H1 1.401(16), Si1–N1 2.0060(12), Si1–N2 1.8265(12), Si1–N3 1.7369(12), Si1–N3A 1.8037(12), N1–Si1–N2 68.20(5), N1–Si1–N3 100.05(5), N1–Si1–N3A 176.92(5).


© 2024 The Authors. Chemistry - A European Journal published by Wiley-VCH GmbH

15213765, 2024, 31, Downloaded from https://chemistry-europe.onlinelibrary.wiley.com/doi/10.1002/chem.202400389, Wiley Online Library on [07/11/2026]. See the Terms and Conditions (https://onlinelibrary.wiley.com/terms-and-conditions) on Wiley Online Library for rules of use; OA articles are governed by the applicable Creative Commons License

space group $P\bar{1}$ with half a molecule in the asymmetric unit. The structure demonstrates that both silicon atoms adopt a trigonal-bipyramidal arrangement with two amidinate nitrogen atoms (N1 and N3a) occupying the axial positions and two nitrogen atoms (N2 of the amidinate and N3 of the *p*-toluidine) as well as the hydride ligand H1 occupying the equatorial positions. The position of the latter was taken from the difference Fourier maps and refined freely. The trigonal-bipyramidal geometry of the silicon atoms in **2** is further supported by the almost linear axial N1–Si–N3a bond angle of 176.92(5)° and the sum of the equatorial bond angles close to 360° (357.7°). The relatively long axial Si1–N1 bond of 2.0060(12) Å compared to the other two (Si1–N2 1.8265(12) and Si1–N3 A 1.8037(12) Å) indicates one of the axial nitrogen atoms of the amidinate to form a dative bond to the silicon atom, which is also supported by DFT studies (*vide infra*). The angle between the four-membered $Si_2N_2$ ring and the $CN_2Si$ ring planes is 60.27(5)°, probably to avoid steric congestion caused by bulky $^t$Bu groups (see SI: Figure S19). The striking feature of **2** is the presence of two Si–H bonds *trans* to each other, suggesting its further utility in various reactions.

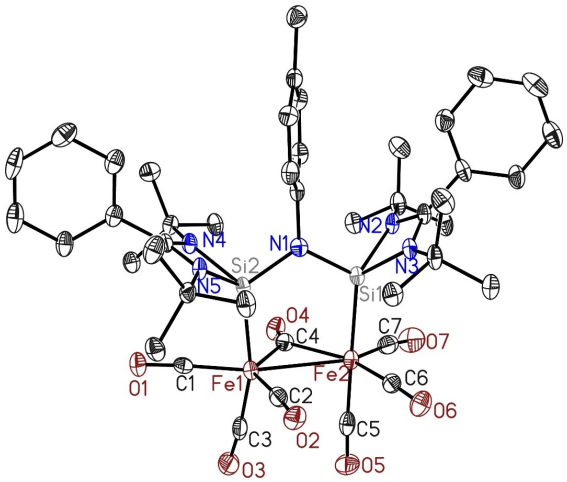
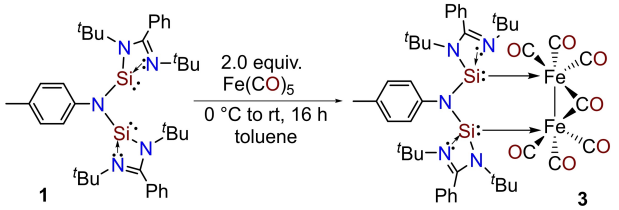



**Figure 6.** Molecular structure of **3**. The anisotropic displacement parameters are depicted at the 50% probability level. Hydrogen atoms have been omitted for clarity. Selected bond lengths (Å) and bond angles (°). Fe1–Si2 2.2525(17), Fe2–Si1 2.2972(18), Si1–Si2 2.982(2), Fe1–Fe2 2.6892(13), Si1–N1 1.740(5), Si1–N2 1.875(5), Si1–N3 1.850(4), Si2–N1 1.736(5), Si2–N4 1.855(4), Si2–N5 1.845(5), Fe2–C from 1.741(6) (C7) to 2.042(5) (C4), Fe1–C from 1.742(5) (C1) to 1.945(5) (C4), Si2–N1–Si1 118.2(2), N1–Si1–Fe2 115.98(16), N1–Si2–Fe1 118.30(16), Fe1–C4–Fe2 84.8(2), Si1–Fe2–C5 178.73(19), Si2-Fe1-Fe2 93.39(5).

## Synthesis of Fe(0) Complex 3

While iron complexes with monosilylene ligands have been studied, there are only a few examples on iron complexes with bis(silylenes) ligands.[19] Based on this knowledge and with bis(silylene)-based ligand **1** in hand, we investigated its coordination ability to Fe(0). Surprisingly, the reaction of **1** with two equivalents of $Fe(CO)_5$ in toluene under an atmospheric pressure of argon gas gave a deep red-coloured solution, from which complex **3** was obtained in 78% yield. As shown in Scheme 3 compound **1** reacts with two molecules of $Fe(CO)_5$ and three labile CO ligands are released. Two Fe atoms form a Fe–Fe bond supported by one μ-bridging CO ligand to form an interesting $NSi_2Fe_2$ five-membered ring. Notably, we also performed this reaction with only one equivalent of $Fe(CO)_5$, but the same complex **3** was formed. The $^{29}$Si NMR spectra of **3** (Figure S13) showed a singlet resonance at 36.51 ppm, which is significantly downfield shifted (46 ppm) compared to **1** and is in agreement with the transition metal carbonyl complexes stabilized by bis(silylene) ligands.[19b]

The X-ray structure (Figure 6) shows that complex **3** crystallizes in the triclinic space group $P\bar{1}$ with one molecule in the asymmetric unit. In the molecular structure of **3** the bis(NHSi) ligand **1** and one CO ligand are bridging the $(CO)_3Fe–Fe(CO)_3$ moiety, yielding an 18-electron complex. The $Si^{II}\cdots Si^{II}$ distance is not noticeably affected by the coordination to Fe(0). However, the Si–N–Si bite angle opens up and becomes considerably large (118.2(2)°) when compared to the free ligand **1** (109.33(8)°) to accommodate two Fe atoms. The Fe–Fe bond distance is 2.6892(13) Å and hence in the range of Fe–Fe bond lengths (2.13–2.73 Å) found in similar molecules. The Si–Fe bond distances are approximately the same, 2.2525(17) and 2.2972(18) Å, and are similar to iron carbonyl complexes of amidinato-silylenes.[19b–d,20] The IR spectrum of **3** showed CO stretching frequencies in the 2056 to 1851 $cm^{-1}$ range (see SI: Figure S16). The terminal CO stretching frequencies (2056-1929 $cm^{-1}$) in **3** are similar to the same found in $[(PhC(N^tBu)_2)(O^tBu)Si{:}\rightarrow Fe(CO)_4]$[19d] (2026–1899 $cm^{-1}$) and $[\{Me_2NC(N^tBu)(NDipp)\}(H)Si{:}\rightarrow Fe(CO)_4]$[20a] (2022–1909 $cm^{-1}$) complexes. However, as expected, the $\mu_2$-bridging CO was slightly shifted to lower frequency and appeared at 1851 $cm^{-1}$, similar to those reported for $\mu_2$-bridged CO transition metal complexes.[21]




**Scheme 3.** Synthesis of Fe(0) complex **3**.

## Theoretical Studies

To explore the structural and bonding aspects for **1–3**, we have performed Density Functional Theoretical (DFT) calculations with the Gaussian16 software[22] on optimized (**1** and **2**, B3LYP–D3/TZVP for Si and B3LYP–D3/SVP for N, C and H; Table S6) and XRD (**3**) structures.[23] Second-order perturbation theory analysis of fock matrix in natural bonding orbital (NBO)[24] basis (B3LYP–D3/def2-TZVP[25] for Si and Fe, and B3LYP–D3/def2-SVP for O, N, C and H) on **1–3** suggest strongest Si···Si interaction for **3** {$Si(3s3p_{x/y})$ - $Si(3s3p_{x/y})$} followed by **2**


© 2024 The Authors. Chemistry - A European Journal published by Wiley-VCH GmbH

15213765, 2024, 31, Downloaded from https://chemistry-europe.onlinelibrary.wiley.com/doi/10.1002/chem.202400389, Wiley Online Library on [07/11/2026]. See the Terms and Conditions (https://onlinelibrary.wiley.com/terms-and-conditions) on Wiley Online Library for rules of use; OA articles are governed by the applicable Creative Commons License

{Si(3s3p$_{y/z}$)–Si(3s3p$_{y/z}$)} and **1** {Si(3s3p$_z$) - Si(3s3p$_{x/z}$)}, respectively (Figure S21). This strong Si···Si interaction for **3** can be attributed to strong back bonding from Fe (3s4p$_x$3d$_{z^2/xz}$) to Si (3s3p$_{x/y}$). This is further supported by the NBO orbital composed of Fe1(4p$_x$3d$_{z^2}$)-Fe2(4p$_x$3d$_{xz}$) with electronic occupation 1.309, due to its involvement in the electron donation (Figure 7a–c and S22). While the Si···Si distance in **2** is shorter than in **1** and **3**, the N–H activation of *p*-toluidine across Si atoms leads to the formation of the Si–H bond in **2** (Figure 7d) and thus weakening of Si···Si interaction. NBO analysis further suggests two strong and different Si–N(*p*-toluidine) bond types in **2**. This is further supported by Atoms In Molecules (AIM) analysis[26] (Figure 8 and Table S7, electron density of $\rho_{(SiN)} = 0.50$ and 0.38 e Bohr$^{-3}$) and expected because **2** has two different types of Si–N1 bonds. AIM analysis further suggests that **3** has the strongest Si–N interaction (electron density of $\rho_{(Si\text{-}N)} = 0.54$ and 0.55 e Bohr$^{-3}$) followed by **2** and **1** (electron density of $\rho_{(Si\text{-}N)} = 0.41$ e Bohr$^{-3}$). DFT estimated the highest occupied molecular orbital (HOMO) for **1** to be a π*-type orbital centered on the aromatic *p*-toluidine group and the Si atoms with a prominent contribution from the 3s orbital (Figure 9). This suggests reactivity of **1** toward *p*-toluidine and Fe(CO)$_5$ leading to the formation of **2** and **3** respectively. In contrast, **2** has the HOMO localized on the *p*-toluidine group. For **3**, the HOMO is centered at the Fe$_2$(CO)$_7$ moiety where the carbonyl-π* orbitals interact with the Fe1(d$_{z^2}$)/Fe2(d$_{x^2-y^2}$) orbitals. The LUMOs for **1**–**3** are centered on the aromatic rings of the heteroleptic silylenes and are of π*-type.

## Conclusions

In conclusion, we have successfully synthesized a tight-bite bis(NHSi) ligand **1** and studied its reactivity in the N–H bond

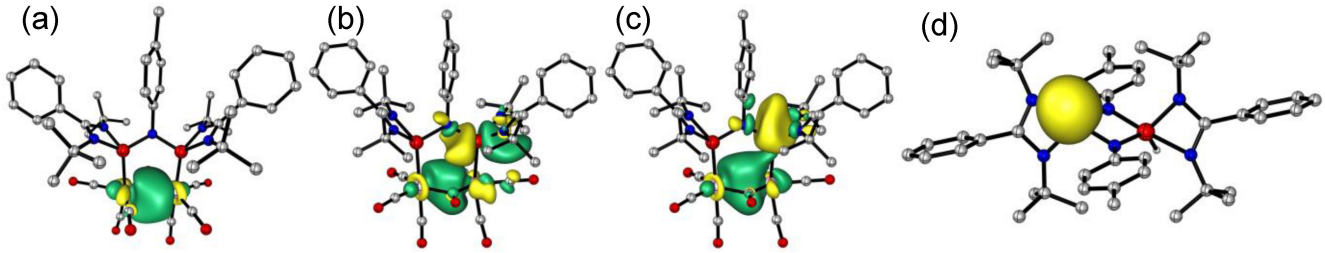



**Figure 7.** DFT computed NBO based (a) molecular orbital for **3** depicting a strong Fe–Fe interaction {Fe1(4p$_x$)$^{0.42}$(3d$_{z^2}$)$^{0.52}$ - Fe2(4p$_x$)$^{0.46}$(3d$_{xz}$)$^{0.46}$} with an electron population of 1.309; (b, c) NBO computed donor-acceptor plots for [{Fe1(4p$_x$3d$_{z^2}$)$^{0.57}$ - Fe2(4p$_x$3d$_{xz}$)$^{0.43}$}→{Si2(3p$_x$)$^{1.0}$}] = 28.1 kcal/mol and [{Fe1(4p$_x$3d$_{z^2}$)$^{0.57}$ - Fe2(4p$_x$3d$_{xz}$)$^{0.43}$}→{Si2(3s3p$_y$)$^{1.0}$}] = 12.8 kcal/mol, respectively; (d) NBO based molecular orbital for **2** depicting the Si–H bonding {Si(3s)$^{0.45}$(3p$_z$)$^{0.55}$ - H(1 s)$^{1.00}$} with an electron population of 1.977.

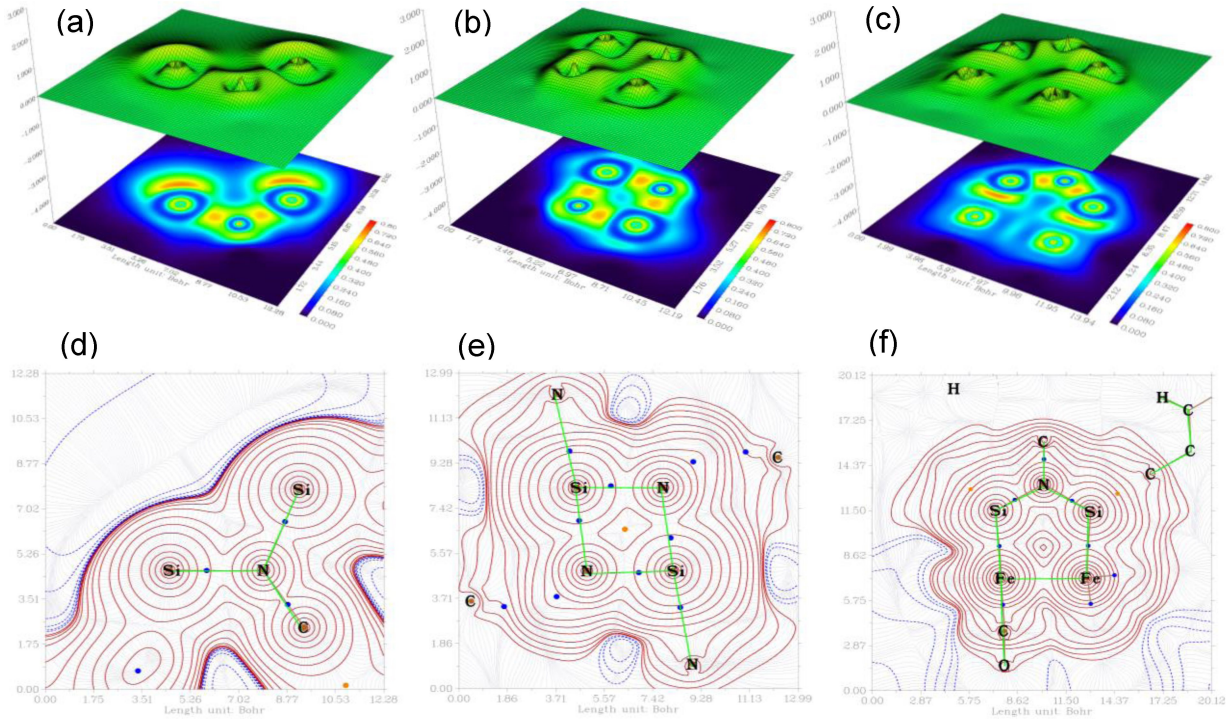



**Figure 8.** DFT-QTAIM computed (a-c) shaded surface maps for **1**–**3**, respectively, showing localized orbital locator (LOL) and (d-f) contour maps for **1**–**3**, respectively, showing molecular electrostatic potential (ESP).


© 2024 The Authors. Chemistry - A European Journal published by Wiley-VCH GmbH

15213765, 2024, 31, Downloaded from https://chemistry-europe.onlinelibrary.wiley.com/doi/10.1002/chem.202400389, Wiley Online Library on [07/11/2026]. See the Terms and Conditions (https://onlinelibrary.wiley.com/terms-and-conditions) on Wiley Online Library for rules of use; OA articles are governed by the applicable Creative Commons License

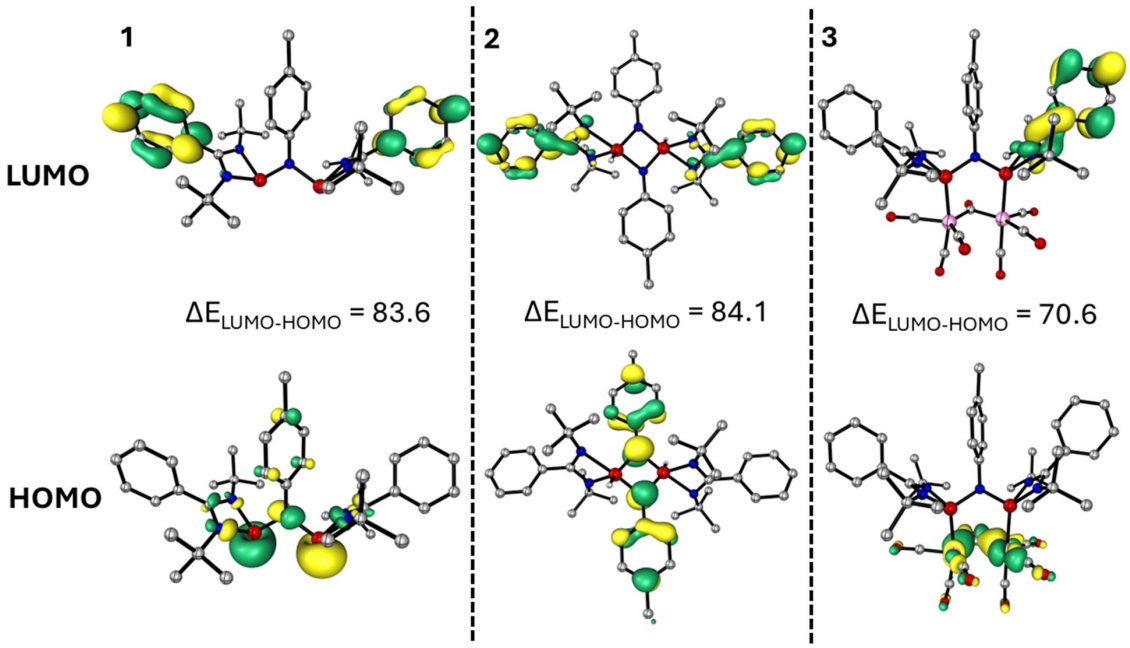



**Figure 9.** DFT computed HOMO-LUMO orbitals for **1**–**3** along with the energy difference ($\Delta E_{LUMO\text{-}HOMO}$) in kcal/mol.

activation of *p*-toluidine and in complexation with a Fe(0) precursor. The first reaction led to the oxidative addition of both N–H bonds of *p*-toluidine at each silicon(II) atom, resulting in the formation of a four-membered cyclodisilazane containing two Si–H functions. In the case of the Fe complex **3**, ligand **1** acts as a μ-bridging A-frame ligand and affords an interesting binuclear complex with Fe–Fe bond by expanding its bite angle to incorporate two metals. The DFT calculations suggest the strongest Si···Si interaction in complex **3** owing to a back donation from Fe(0) to Si(II) atoms. This study highlights the potential of bissilylenes as versatile building blocks in bond-activation reactions and other applications, warranting further investigations in this rapidly evolving field of chemistry.

## Experimental section

**General Comments**. All manipulations were performed under an Ar atmosphere using Schlenk techniques. [PhC(N$^t$Bu)$_2$SiCl] was prepared according to the previous literature,[4b] and all solvents were purchased from commercial sources. The solvents were dried and distilled over suitable agents before use. $^1$H, $^{13}$C{1H}, and $^{29}$Si NMR spectra were recorded on a Bruker Avance 400 MHz instrument. Chemical shifts are reported in parts per million (ppm) and are referenced to residual peaks of the deuterated solvents. High-resolution mass spectra were measured on a Bruker Daltonik MaXis ESI-QTOF instrument.

**Synthesis of 1**. $^n$BuLi (2 mL, 2.5 M in hexanes) was added dropwise to the solution of *p*-toluidine (0.5 g, 4.66 mmol) in toluene (45 mL) at −85 °C and the resulting mixture was allowed to warmed to ambient temperature and was further stirred for 4 h. Subsequently the reaction mixture was cooled again to −85 °C and a solution of [(PhC(N$^t$Bu)$_2$SiCl] (2.751 g, 9.32 mmol) in toluene (20 mL) was added dropwise. The reaction mixture was slowly warmed to ambient temperature and stirred for another 16 h. Then it was filtered to remove LiCl, and the solvents were removed under *vacuum* to give compound **1** as a dark yellow solid. This was washed twice with 5 mL of hexane to afford the pure product as a bright yellow solid. Single crystals of **1** suitable for X-ray diffraction analysis were grown by slow evaporation of the toluene solution at room temperature over one week at −20 °C. Yield 2.03 g (70%). mp 182 °C(dec.). $^1$H NMR (400 MHz, $C_6D_6$); δ = 7.38 (t, *J* = 4.4 Hz, 4H, ArH), 7.26 (d, *J* = 7.8 Hz, 2H, ArH), 7.12 (d, *J* = 7.3 Hz, 1H, ArH), 7.08 (d, *J* = 7.8 Hz, 2H, ArH), 7.02 (t, *J* = 8.4 Hz, 1H, ArH), 7.00–6.93 (m, 4H, ArH), 6.94–6.87 (m, 2H, ArH), 2.34 (s, 3H, ArCH$_3$), 1.20 (s, 36H, N$^t$Bu). $^{13}$C NMR (101 MHz, $C_6D_6$): δ = 161.13 (s, $^t$BuN<u>C</u>N$^t$Bu), 147.75 (s, Ar<u>C</u>), 135.03 (s, Ar<u>C</u>), 130.70 (s, Ar<u>C</u>), 129.37 (s, Ar<u>C</u>), 129.33 (s, Ar<u>C</u>), 129.20 (s, Ar<u>C</u>), 128.58 (s, Ar<u>C</u>), 128.23 (s, Ar<u>C</u>), 127.70 (s, Ar<u>C</u>), 127.52 (s, Ar<u>C</u>), 125.70 (s, Ar<u>C</u>), 123.87 (s, Ar<u>C</u>), 53.01 (brs, <u>C</u>Me$_3$), 31.72 (brs, C<u>Me</u>$_3$), 21.16 (s, Ar<u>C</u>H$_3$). $^{29}$Si NMR (80 MHz, $C_6D_6$); δ = -12.24 (s). MS (LIFDI, toluene): m/z for $C_{37}H_{53}N_5Si_2$ (M)$^+$: 623.4

**Synthesis of 2**. To the solution of bis(NHSi) (**1**) (0.300 g, 0.48 mmol) in toluene (30 mL), a solution of *p*-toluidine (0.051 g, 0.48 mmol), also in toluene (40 mL), was added dropwise at room temperature. The reaction mixture was stirred for another three days at the same temperature. During this time the yellow solution turned colorless. The solvents were removed under *vacuum*, and the resulting solid was washed with hexane (2 x 15 mL) to give the product as an off-white solid. Single crystals suitable for X-ray diffraction analysis were grown from slow evaporation of a toluene solution of **2** at room temperature over one week. Yield 72% (0.252 g). mp = 252-256 °C (dec.). $^1$H NMR (400 MHz, $C_6D_6$): δ = 7.58 (d, *J* = 7.8 Hz, 4H, ArH), 7.30 (t, *J* = 6.6 Hz, 8H, ArH), 6.97 (d, *J* = 7.1 Hz, 6H, ArH), 6.20 (s, 2H, SiH), 2.35 (s, 6H, ArCH$_3$), 1.50–1.34 (m, 18H, $^t$Bu), 0.96 (s, 18H, $^t$Bu). $^{13}$C NMR (101 MHz, THF-$D_8$): δ = 169.67 (s, $^t$BuN<u>C</u>N$^t$Bu), 148.65 (s, Ar<u>C</u>), 137.47 (s, Ar<u>C</u>), 130.91 (s, Ar<u>C</u>), 130.62 (s, Ar<u>C</u>), 129.26 (s, Ar<u>C</u>), 129.07 (s, Ar<u>C</u>), 128.56 (s, Ar<u>C</u>), 127.80 (s, Ar<u>C</u>), 124.59 (s, Ar<u>C</u>), 54.93 (brs, <u>C</u>Me$_3$), 32.71 (brs, C<u>Me</u>$_3$), 31.69 (brs, C<u>Me</u>$_3$), 21.15 (Ar<u>C</u>H$_3$). $^{29}$Si{$^1$H} NMR (80 MHz, $C_6D_6$); δ = −97.84 (s). MS (LIFDI, toluene): m/z for $C_{44}H_{62}N_6Si_2$ (M)$^+$: 730.3.

**Synthesis of 3**. It was prepared by adding two equivalents of $Fe(CO)_5$ (86.6 μL, 0.64 mmol) to a solution of **1** (200 mg, 0.32 mmol) in 50 mL of freshly distilled dry toluene at 0 °C. The mixture turned


© 2024 The Authors. Chemistry - A European Journal published by Wiley-VCH GmbH

15213765, 2024, 31, Downloaded from https://chemistry-europe.onlinelibrary.wiley.com/doi/10.1002/chem.202400389, Wiley Online Library on [07/11/2026]. See the Terms and Conditions (https://onlinelibrary.wiley.com/terms-and-conditions) on Wiley Online Library for rules of use; OA articles are governed by the applicable Creative Commons License

to a dark red solution immediately. It was stirred for 8 hours. Subsequently the solvent was reduced under *vacuum* to 5 mL and kept at −18 °C to give the pure crystalline red product. Crystals suitable for X-ray diffraction analysis were grown by slow evaporation of the $C_6D_6$ solution at 20 °C. Yield 66%. mp 238–240 °C-(dec.).$^1$H NMR (400 MHz, $C_6D_6$): δ = 7.40 (d, 1H, ArH), 7.27-7.24 (m, 10H, ArH), 7.08-7.00 (m, 3H, ArH), 2.32 (s, 3H, $-CH_3$), 1.34 (s, 36H, $-{}^tBu$). $^{13}$C NMR (101 MHz, $C_6D_6$): δ = 210.10 (s, CO), 152.64 (s, $^tBuNCN^tBu$), 140.44 (s, ArC), 139.85 (s, ArC), 132.81 (s, ArC), 129.71 (s, ArC), 129.53 (s, ArC), 129.30 (s, ArC), 129.10 (s, ArC), 128.12 (s, ArC), 127.64 (s, ArC), 116.91 (s, ArC), 115.95 (s, ArC), 52.79 (brs, $CMe_3$), 51.21 (brs, $CMe_3$), 25.20 (s, $CMe_3$), 20.46 (s, $ArCH_3$). $^{29}$Si NMR (400 MHz, $C_6D_6$): δ 36.51 (s). MS (LIFDI, toluene): m/z for $C_{44}H_{53}N_5O_7Si_2Fe_2$ $(M)^+$: 931.2.

### Crystal Structure Determination

The diffraction data were collected using Mo Kα radiation and a Bruker Photon III detector (**2** and **3**) and Ag Kα radiation and a Bruker Apex II detector (**1**). The data were integrated with SAINT.[9a] A multi-scan absorption correction was applied using SADABS[9b] (**2** and **3**) and TWINABS[27] (**1**). A 3λ correction was applied for structure **2**.[9b] The structures were solved by SHELXT[9d] and refined on $F^2$ using SHELXL[9c] in the graphical user interface ShelXle.[9e] All hydrogen atoms were placed according to geometrical criteria and refined with a riding model, except for H1 in **2**, which was refined freely. In structure **1**, a severely disordered toluene molecule on a special position was treated using SQUEEZE.[28]

## Supporting Information

Data that support the findings of this study are available in the Supporting Information of this article.

Deposition Numbers 2326411 (for **1**), 2326412 (for **2**), and 2326413 (for **3**), contain the supplementary crystallographic data for this paper. These data are provided free of charge by the joint Cambridge Crystallographic Data Centre and Fachinformationszentrum Karlsruhe Access Structures service.

## *Acknowledgements*

K.R. and D.St. thank the GRK BENCh, which is funded by the Deutsche Forschungsgemeinschaft (DFG, German Research Foundation) - 389479699/GRK2455. Open Access funding enabled and organized by Projekt DEAL.

## *Conflict of Interests*

The authors declare no conflict of interest.

## *Data Availability Statement*

The data that support the findings of this study are available in the supplementary material of this article.

**Keywords:** bissilylene · N-heterocyclic silylene · transition metals · chelating ligands · structure determination

[1] a) R. S. Ghadwal, R. Azhakar, H. W. Roesky, *Acc. Chem. Res.* **2013**, *46*, 444–456; b) M. Haaf, T. A. Schmedake, R. West, *Acc. Chem. Res.* **2000**, *33*, 704–714; c) S. Yao, A. Saddington, Y. Xiong, M. Driess, *Acc. Chem. Res.* **2023**, *56*, 475–488.
[2] M. Denk, R. Lennon, R. Hayashi, R. West, A. V. Belyakov, H. P. Verne, A. Haaland, M. Wagner, N. Metzler, *J. Am. Chem. Soc.* **1994**, *116*, 2691–2692.
[3] a) B. Blom, D. Gallego, M. Driess, *Inorg. Chem. Front.* **2014**, *1*, 134–148; b) B. Blom, M. Stoelzel, M. Driess, *Chem. Eur. J.* **2013**, *19*, 40–62; c) L. Wang, Y. Li, Z. Li, M. Kira, *Coord. Chem. Rev.* **2022**, *457*, 214413; d) C. Shan, S. Yao, M. Driess, *Chem. Soc. Rev.* **2020**, *49*, 6733–6754; e) M. Ghosh, S. Khan, *Dalton Trans.* **2021**, *50*, 10674–10688.
[4] a) C.-W. So, H. W. Roesky, J. Magull, R. B. Oswald, *Angew. Chem. Int. Ed.* **2006**, *45*, 3948–3950; b) S. S. Sen, H. W. Roesky, D. Stern, J. Henn, D. Stalke, *J. Am. Chem. Soc.* **2010**, *132*, 1123–1126.
[5] a) S. S. Sen, A. Jana, H. W. Roesky, C. Schulzke, *Angew. Chem. Int. Ed.* **2009**, *48*, 8536–8538; b) S. S. Sen, S. Khan, P. P. Samuel, H. W. Roesky, *Chem. Sci.* **2012**, *3*, 659–682; c) Y. Zhang, L. Wu, H. Wang, *Coord. Chem. Rev.* **2023**, *477*, 214942; d) J. Xu, C. Dai, S. Yao, J. Zhu, M. Driess, *Angew. Chem. Int. Ed.* **2022**, *61*, e202114073; e) Y. Wang, M. Karni, S. Yao, A. Kaushansky, Y. Apeloig, M. Driess, *J. Am. Chem. Soc.* **2019**, *141*, 12916–12927; f) S. Yao, Y. Xiong, A. Saddington, M. Driess, *Chem. Commun.* **2021**, *57*, 10139–10153; g) Y. Wang, T. Szilvási, S. Yao, M. Driess, *Nat. Chem.* **2020**, *12*, 801–807.
[6] a) S. S. Sen, S. Khan, S. Nagendran, H. W. Roesky, *Acc. Chem. Res.* **2012**, *45*, 578–587; b) W. Wang, S. Inoue, S. Yao, M. Driess, *J. Am. Chem. Soc.* **2010**, *132*, 15890–15892.
[7] Y. Xiong, S. Dong, S. Yao, C. Dai, J. Zhu, S. Kemper, M. Driess, *Angew. Chem. Int. Ed.* **2022**, *61*, e202209250.
[8] Y. Xiong, S. Dong, S. Yao, C. Lorent, K. B. Krause, G. Vijaykumar, J. Zhu, C. Limberg, M. Driess, *Nat. Synth* **2023**, *2*, 678–687.
[9] a) S. v. A. Bruker AXS Inc., Madison, **2016**; b) L. Krause, R. Herbst-Irmer, G. M. Sheldrick, D. Stalke, *J. Appl. Crystallogr.* **2015**, *48*, 3–10; c) G. Sheldrick, *Acta Crystallogr.* **2015**, *C71*, 3–8; d) G. Sheldrick, *Acta Crystallogr.* **2015**, *A71*, 3–8; e) C. B. Hübschle, G. M. Sheldrick, B. Dittrich, *J. Appl. Crystallogr.* **2011**, *44*, 1281–1284.
[10] a) J. L. Klinkenberg, J. F. Hartwig, *Angew. Chem. Int. Ed.* **2011**, *50*, 86–95; b) V. Krishnakumar, B. Chatterjee, C. Gunanathan, *Inorg. Chem.* **2017**, *56*, 7278–7284; c) K. Muñiz, A. Lishchynskyi, J. Streuff, M. Nieger, E. C. Escudero-Adán, M. M. Belmonte, *Chem. Commun.* **2011**, *47*, 4911–4913.
[11] J. I. van der Vlugt, *Chem. Soc. Rev.* **2010**, *39*, 2302–2322.
[12] T. Chu, G. I. Nikonov, *Chem. Rev.* **2018**, *118*, 3608–3680.
[13] S. Fujimori, S. Inoue, *Eur. J. Inorg. Chem.* **2020**, *2020*, 3131–3142.
[14] a) A. Jana, C. Schulzke, H. W. Roesky, *J. Am. Chem. Soc.* **2009**, *131*, 4600–4601; b) T. J. Hadlington, J. A. B. Abdalla, R. Tirfoin, S. Aldridge, C. Jones, *Chem. Commun.* **2016**, *52*, 1717–1720; c) D. C. H. Do, A. V. Protchenko, M. Á. Fuentes, J. Hicks, P. Vasko, S. Aldridge, *Chem. Commun.* **2020**, *56*, 4684–4687.
[15] S. L. McOnie, G. A. Özpınar, J. L. Bourque, T. Müller, K. M. Baines, *Dalton Trans.* **2021**, *50*, 17734–17750.
[16] a) C. Neumann, A. Schulz, T. Seifert, W. Storch, M. Vosteen, *Eur. J. Inorg. Chem.* **2002**, *2002*, 1040–1045; b) D. R. Armstrong, D. Barr, W. Clegg, S. R. Drake, R. J. Singer, R. Snaith, D. Stalke, D. S. Wright, *Angew. Chem. Int. Ed.* **1991**, *30*, 1707–1709.
[17] a) B. Jaschke, R. Herbst-Irmer, U. Klingebiel, P. Neugebauer, T. Pape, *J. Chem. Soc. Dalton Trans.* **1998**, 2953–2954; b) S. Khan, S. S. Sen, R. Michel, D. Kratzert, H. W. Roesky, D. Stalke, *Organometallics* **2011**, *30*, 2643–2645; c) S. P. Sarish, A. Jana, H. W. Roesky, P. P. Samuel, C. E. A. Andrade, B. Dittrich, C. Schulzke, *Organometallics* **2011**, *30*, 912–916.
[18] a) F. M. Mück, J. A. Baus, C. Burschka, R. Tacke, *Chem. Eur. J.* **2016**, *22*, 5830–5834; b) S. Metz, C. Burschka, D. Platte, R. Tacke, *Angew. Chem. Int. Ed.* **2007**, *46*, 7006–7009; c) J. A. Baus, C. Burschka, R. Bertermann, C. F. Guerra, F. M. Bickelhaupt, R. Tacke, *Inorg. Chem.* **2013**, *52*, 10664–10676.
[19] a) P. Garg, A. Carpentier, I. Douair, D. Dange, Y. Jiang, K. Yuvaraj, L. Maron, C. Jones, *Angew. Chem. Int. Ed.* **2022**, *61*, e202201705; b) S. K. Kushvaha, P. Kallenbach, S. M. N. V. T. Gorantla, R. Herbst-Irmer, D. Stalke, H. W. Roesky, *Chem. Eur. J.* **2023**, *n/a*, e202303113; c) M. K. Pandey, Z. Hendi, X. Wang, A. Bhandari, M. K. Singh, K. Rachuy, S. K. Kushvaha, R. Herbst-Irmer, D. Stalke, H. W. Roesky, *Angew. Chem. Int. Ed.* **2023**, *n/a*, e202317416; d) W. Yang, H. Fu, H. Wang, M. Chen, Y. Ding, H. W. Roesky, A. Jana, *Inorg. Chem.* **2009**, *48*, 5058–5060.


© 2024 The Authors. Chemistry - A European Journal published by Wiley-VCH GmbH

15213765, 2024, 31, Downloaded from https://chemistry-europe.onlinelibrary.wiley.com/doi/10.1002/chem.202400389, Wiley Online Library on [07/11/2026]. See the Terms and Conditions (https://onlinelibrary.wiley.com/terms-and-conditions) on Wiley Online Library for rules of use; OA articles are governed by the applicable Creative Commons License

[20] a) B. Blom, M. Pohl, G. Tan, D. Gallego, M. Driess, *Organometallics* **2014**, *33*, 5272–5282; b) R. Tacke, C. Kobelt, J. A. Baus, R. Bertermann, C. Burschka, *Dalton Trans.* **2015**, *44*, 14959–14974.
[21] R. Colton, M. J. McCormick, *Coord. Chem. Rev.* **1980**, *31*, 1–52.
[22] M. J. Frisch, G. W. Trucks, H. B. Schlegel, G. E. Scuseria, M. A. Robb, J. R. Cheeseman, G. Scalmani, V. Barone, G. A. Petersson, H. Nakatsuji, X. Li, M. Caricato, A. V. Marenich, J. Bloino, B. G. Janesko, R. Gomperts, B. Mennucci, H. P. Hratchian, J. V. Ortiz, A. F. Izmaylov, J. L. Sonnenberg, Williams, F. Ding, F. Lipparini, F. Egidi, J. Goings, B. Peng, A. Petrone, T. Henderson, D. Ranasinghe, V. G. Zakrzewski, J. Gao, N. Rega, G. Zheng, W. Liang, M. Hada, M. Ehara, K. Toyota, R. Fukuda, J. Hasegawa, M. Ishida, T. Nakajima, Y. Honda, O. Kitao, H. Nakai, T. Vreven, K. Throssell, J. A. Montgomery Jr., J. E. Peralta, F. Ogliaro, M. J. Bearpark, J. J. Heyd, E. N. Brothers, K. N. Kudin, V. N. Staroverov, T. A. Keith, R. Kobayashi, J. Normand, K. Raghavachari, A. P. Rendell, J. C. Burant, S. S. Iyengar, J. Tomasi, M. Cossi, J. M. Millam, M. Klene, C. Adamo, R. Cammi, J. W. Ochterski, R. L. Martin, K. Morokuma, O. Farkas, J. B. Foresman, D. J. Fox, Gaussian 16, Revision C.01, Wallingford, CT, **2016**.
[23] a) A. D. Becke, *Phys. Rev. A* **1988**, *38*, 3098–3100; b) A. D. Becke, *J. Chem. Phys.* **1993**, *98*, 5648–5652; c) C. Lee, W. Yang, R. G. Parr, *Phys. Rev. B* **1988**, *37*, 785–789; d) S. Grimme, J. Antony, S. Ehrlich, H. Krieg, *J. Chem. Phys.* **2010**, *132*, 154104; e) A. Schäfer, H. Horn, R. Ahlrichs, *J. Chem. Phys.* **1992**, *97*, 2571–2577; f) A. Schäfer, C. Huber, R. Ahlrichs, *J. Chem. Phys.* **1994**, *100*, 5829–5835.
[24] a) J. P. Foster, F. Weinhold, *J. Am. Chem. Soc.* **1980**, *102*, 7211–7218; b) M. K. Singh, N. Yadav, G. Rajaraman, *Chem. Commun.* **2015**, *51*, 17732–17735.
[25] F. Weigend, R. Ahlrichs, *Phys. Chem. Chem. Phys.* **2005**, *7*, 3297–3305.
[26] a) T. Lu, F. Chen, *J. Comput. Chem.* **2012**, *33*, 580–592; b) H. L. Schmider, A. D. Becke, *J. Mol. Struc-THEOCHEM* **2000**, *527*, 51–61.
[27] M. Sevvana, M. Ruf, I. Uson, G. M. Sheldrick, R. Herbst-Irmer, *Acta Crystallogr.* **2019**, *D75*, 1040–1050.
[28] A. Spek, *Acta Crystallogr.* **2015**, *C71*, 9–18.

Manuscript received: January 29, 2024
Accepted manuscript online: March 17, 2024
Version of record online: April 8, 2024


© 2024 The Authors. Chemistry - A European Journal published by Wiley-VCH GmbH

15213765, 2024, 31, Downloaded from https://chemistry-europe.onlinelibrary.wiley.com/doi/10.1002/chem.202400389, Wiley Online Library on [07/11/2026]. See the Terms and Conditions (https://onlinelibrary.wiley.com/terms-and-conditions) on Wiley Online Library for rules of use; OA articles are governed by the applicable Creative Commons License